

## FRIB BEAM POSITION MONITOR PICK-UP DESIGN\*

Oren Yair<sup>#</sup>, Jenna Crisp, Gerlind Kiupel, Steven Michael Lidia, Robert C. Webber, Facility for Rare Isotope Beams (FRIB), Michigan State University, East Lansing, MI 48824 USA

### Abstract

The heavy ion linac under construction at Michigan State University as part of the Facility for Rare Isotope Beams requires a Beam Position Monitoring System with dual-plane pick-ups at 147 locations. Four different pick-up designs will be used with apertures of 40, 50, 100, and 150 mm. The 40 mm BPMs are designed to operate at cryogenic temperatures, as 39 are bolted to superconducting RF cavities and reside in the insulating vacuum of the cryomodule. The other designs serve only room temperature locations. Requirements, designs, analyses, tests, and status is reported

### INTRODUCTION

The Facility for Rare Isotope Beams (FRIB) will be a new national user facility for nuclear science, funded by the Department of Energy Office of Science (DOE-SC), Michigan State University (MSU), and the State of Michigan. Under construction on campus and operated by MSU, FRIB will provide intense beams of heavy ions to produce rare isotopes. A heavy ion superconducting linac capable of accelerating ions up to Uranium with energies higher than 200 MeV/u and beam power up to 400 kilowatts will be used. The primary time structure for beam ranges from 50  $\mu$ s pulses at 1 Hz to nearly CW beam with 100Hz 50  $\mu$ s notches. The bunch rate will be 20.125, 40.25, or 80.5 MHz and the velocity will range from 3.3 to 50% the speed of light.

With 100  $\mu$ A beam current, the required BPM system accuracy is  $\pm 0.4$  mm and resolution is 0.1 mm. Accuracy includes survey errors with respect to the designed beam orbit, linearity and electrical center in the BPM, cable mismatch, amplifier impedance and gain, and receiver errors. Accuracy addresses the ability to thread the beam safely through the linac while preserving aperture. BPM stability reduces the frequency of beam based alignment and aperture scans used to identify and maintain optimum beam orbit.

Resolution is focused on the ability to measure changes

while tuning. This allows measurement of the machine lattice and helps identify irregularities or failures in other accelerator components. The relevant time period for resolution is a day.

The BPM system will also be used to identify optimum accelerating cavity phase by measuring beam time of flight.[1] With 100  $\mu$ A beam current, the required phase accuracy is  $\pm 2$  degrees at 80.5MHz with 0.5 degree resolution.

Beam intensity will be measured with the BPM system as well. Sensitivity to position and bunch length is problematic. Accuracy of a few percent should be possible for reasonable beam conditions.[2][3]

### BPM PICK-UP RESOLUTION

Split plate style BPMs are inherently more linear [4] than button or stripline BPMs. However, split plate and stripline designs require additional complexities to hold the electrodes in position. The single support point characteristic of button BPMs alleviates problems with differential expansion at cryogenic temperatures.

Button BPMs are both non-linear and dependent on the position in the orthogonal plane. A general rule of thumb is that the button width should be about 60° wide leaving a 30° gap between buttons. Buttons with a flat face rather than one that aligns with the inside surface of the BPM aperture are simpler and less expensive to make, yet, provide good response.

Position and resolution near the center of a button bpm of diameter D is estimated below. The  $D/\pi$  scale factor is only an approximation but is reasonably accurate over 1/3<sup>rd</sup> of the aperture.

$$Pos \approx \frac{D}{\pi} \frac{A-B}{A+B} \text{ mm} \quad Pos_N \approx \frac{D}{\pi\sqrt{2}} \frac{V_N}{V_{button}} \text{ mm}$$

The voltage induced on a BPM electrode can be estimated from its geometry, beam current, and button impedance.[5] The image current has equal but opposite charge on the inside of the beam pipe and follows the beam. The image current flowing onto the button as the beam enters the BPM must come off of the button as the beam exits. The time difference is the combination of the beam flight time and the signal delay time across the button. The fraction of image current intercepted by a button is  $d/4D$ . The BPM output is nearly an ideal current source as the voltage induced on the button is not sufficient to change the beam current. For bunches reasonably short compared to the period of the frequency being measured,  $I(\omega) \approx 2I_{avg}$ .

\*This material is based upon work supported by the U.S. Department of Energy Office of Science under Cooperative Agreement DE-SC0000661, the State of Michigan and Michigan State University. Michigan State University designs and establishes FRIB as a DOE Office of Science National User Facility in support of the mission of the Office of Nuclear Physics.

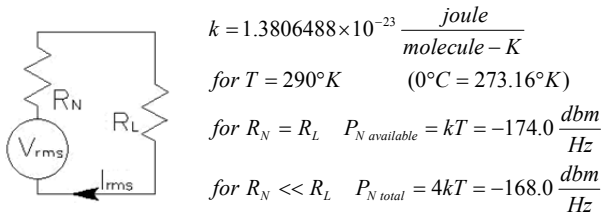
#yair@frib.msu.edu

$$I_{butoff}(t) \approx \frac{d}{4D} \left\{ I_{beam} \left( t + \frac{\Delta t}{2} \right) - I_{beam} \left( t - \frac{\Delta t}{2} \right) \right\} \quad \Delta t = \frac{d}{c} \left( 1 + \frac{1}{\beta} \right)$$

$$I_{beam}(t) = 2I_{avg} \sin \omega t \quad \sin(\alpha + \beta) - \sin(\alpha - \beta) = 2 \cos \alpha \sin \beta$$

$$V_{butoff}(t) = Z_{butoff} \frac{d}{4D} 2I_{avg} 2 \sin \frac{\omega d}{2c} \left( 1 + \frac{1}{\beta} \right) \cos \omega t$$

An optimum digital receiver would have sufficient gain so that the error associated with the least significant bit projected to the BPM output is less than that contributed by thermal noise. The total thermal noise power spectral density is provided below. Total noise rather than available noise is appropriate as the BPM equivalent voltage source impedance is small.



The effective number of bits (ENOB) for an analog to digital converter (ADC) provides a good estimate for the equivalent noise level at the input. ENOB is the number of bits required for an ideal ADC to provide the measured signal to noise ratio (SNR) of the part.

$$V_N\ rms = \frac{ENOB}{2} \sqrt{\frac{1}{T} \int_0^T \left( t \frac{2}{T} - 1 \right)^2 dt} = \frac{ENOB}{2\sqrt{3}}$$

Total noise includes the amplifier noise figure, cable loss, ADC error, and thermal noise. The phase and beam current noise levels can be found from the estimated position noise.

$$Pos \approx \frac{D}{\pi} \frac{A-B}{A+B} \text{ mm} \quad Pos_N \approx \frac{D}{\pi\sqrt{2}} \frac{V_N}{V_{butoff}} \text{ mm}$$

$$for V_{butoff} = Q + jI \quad Q \gg I \quad Q_N \ll Q \quad I_N \gg I$$

$$\varphi_N = atan \frac{I + I_N}{Q + Q_N} \approx \frac{I_N}{Q} = \frac{\sqrt{4}V_N}{4V_{butoff}} = \frac{V_N}{2V_{butoff}} \text{ rad}$$

$$\frac{180}{\sqrt{2}D} Pos_N \text{ deg}$$

$$\frac{Int_N}{Int_{avg}} = \frac{\sqrt{4}V_N}{4V_{butoff}} = \frac{\pi}{\sqrt{2}D} Pos_N$$

Fermilab digital receiver	1.4 db cable loss (125ft LDF1-50)
14 bit ADS6445	6 db noise fig
12.12 ENOB	40 db gain at end of cable
-71.2 dbfs SINAD	37000 Hz BW 4.3 uSec tc
78.06061 MHz	856 samples per measurement
2 Vpp at input	52.14 nVrms ADC equiv error at bpm
182 fSec max clock jitter	403.5 nVrms 4kT equiv noise at bpm
	406.9 nVrms total equiv noise at bpm

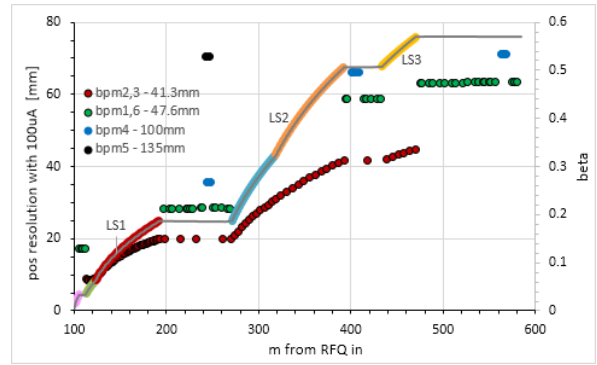


Figure 1: Calculated position resolution for all FRIB BPMs taking into account bandwidth, amplifier gain and noise figure, cable loss, thermal noise, and ADC error.

Figure 1 includes the effect of beam velocity or  $\beta$  in the estimate of image current. For non-relativistic beams, the electric field has an opening angle of about  $1/\gamma$ . A CST studio model was used to determine the image current for a point charge in a round pipe for various beam velocities,  $\sigma_t \approx 0.563D/2\gamma$  as shown in Figs. 2 & 3. [6] For FRIB, the actual bunch length is nearly insignificant for estimating the image current length. The amplitude of the first two rf harmonics, 80.5 and 161MHz are only affected by  $\beta$  in the first 10m of the linac.

A digital receiver with 41.3mm ID BPMs is sufficient to provide the required accuracy and resolution. If necessary, resolution could be improved by limiting the bandwidth at the expense of response time.

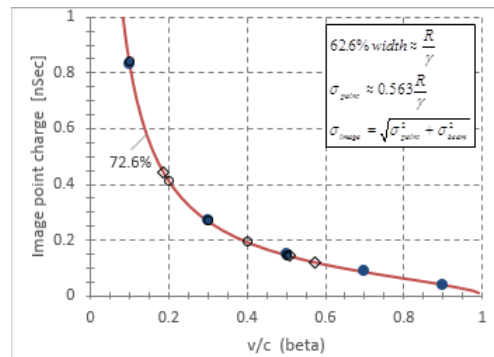


Figure 2: Length of the image current induced by a point charge. CST studio model.

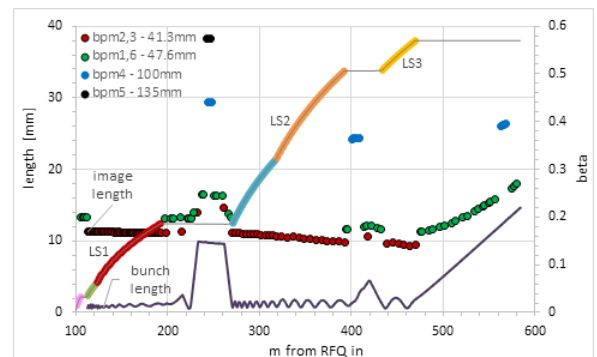


Figure 3: Image current length at all of the FRIB BPMs.

To verify calculation, two prototype BPMs with 35mm aperture and 20mm buttons were installed in ReA3.[7] Fermilab provided digital BPM receivers and interfaced the VME crate running VXWorks to the EPICS control system. Figure 4 shows for each trigger, an array of 2048 measurements each with 37 kHz bandwidth was recorded while beam intensity was scanned from 0.08  $\mu\text{A}$  to 9.6  $\mu\text{A}$ . The standard deviation compares well with the estimate below.

Fermilab digital receiver		1.3 db cable loss (125ft LDF1-50)	
14 bit ADS6445		1 db noise fig	
12.12 ENOB		81 db gain at end of cable	
-71.2 dbfs SINAD		37000 Hz BW	
78.06061 MHz		4.3 uSec tc	
2 Vpp at input		856 samples per measurement	
182 fSec max clock jitter		0.46 nVrms ADC equiv error at bpm	
		224.3 nVrms 4kT equiv noise at bpm	
		224.3 nVrms total equiv noise at bpm	
1 uCoul/sec avg lbeam			
161MHz component, error includes cable, amp, thermal & adc noise			
rms bunch lght 34.9 20 mm dia			
beta	MeV/u	rms deg	image mm
0.04630	1	7.5	10.5
0.08006	3	7.5	11.6
		Vrms-bpm	um-rms
		5.2	336.6
		4.0	445.9
		deg-rms	uA-rms
		1.23	0.086
		1.63	0.114

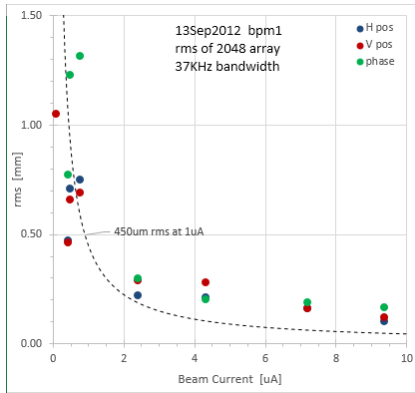


Figure 4: Rms variation in measured beam position in ReA3 for various beam currents. The actual beam measurement matches the estimated value, 450  $\mu\text{m}$  at 1  $\mu\text{A}$ .

## RESULTS

CST studio was used to evaluate methods to correct linearity as shown in Fig. 5. The polynomial has only odd terms for in axis correction (anti-symmetric) and even terms for the orthogonal axis (symmetric). With polynomial correction the error over 2/3rds of the aperture is 50  $\mu\text{m}$  rms.

$$\text{polynomial} \quad D_{bpm} = 41.3\text{mm} \quad d_{but} = 20\text{mm}$$

$$R = \frac{D_{bpm}}{\pi} \frac{a-c}{a+c}$$

$$H_{pos} = p_0 + p_1 R_H + p_3 R_H^3 + p_5 R_H^5 + p_{12} R_H R_V^2 + p_{32} R_H^3 R_V^2$$

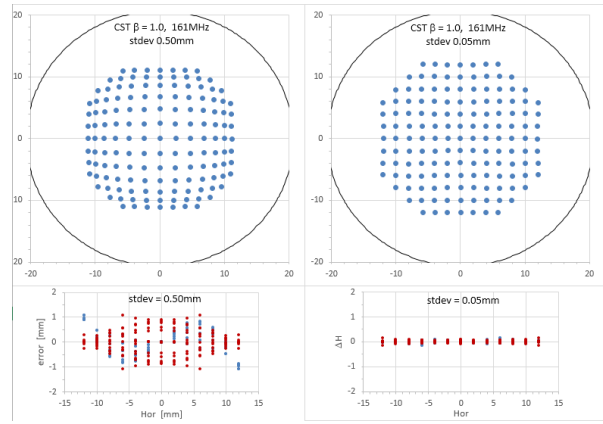


Figure 5: CST studio results with  $\beta = 1.0$ . Linear scaling on left ( $D/\pi$ ) and polynomial scaling on the right. The error is shown in the lower plots.

To validate the CST model 3 of the 4 prototype BPMs were scanned with a wire at Fermilab.[8] Using the same polynomial coefficients the error over 2/3rds the aperture was 80  $\mu\text{m}$  rms for all 3 BPMs at both 80.5 and 161MHz. However, the wire measurement sensitivity was 1.8% higher than our CST model. We compared the CST model with  $\beta = 1$  to the same model but excited with a 1mm wire terminated in 230 $\Omega$  rather than a particle beam. The model using the wire was 1% higher than with a particle beam as shown in Fig. 6. We believe the 1.8% difference is caused by capacitive coupling to the wire.

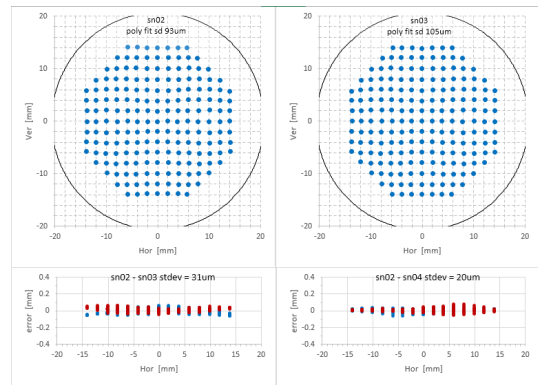


Figure 6: Wire map of sn02 and sn03 BPMs. The rms difference between measured and programmed wire positions is 100  $\mu\text{m}$ . The rms difference between any two wire measurements is less than 50  $\mu\text{m}$ , lower plots.

S One of the acceptance criteria involves measurement of  $\tau_{21}$  between all four buttons. The measurement can be compared to a simple electrical model to reveal the coupling capacitance between buttons and the capacitance to ground as shown in Fig. 7. The 3.3 pF to ground and 50 $\Omega$  load have a corner frequency of 1GHz, well above the 161MHz component used to measure position. The results are kept in the traveler so that the BPM can be evaluated at a later time. We anticipate checking all cold BPMs before sealing the cryomodule.

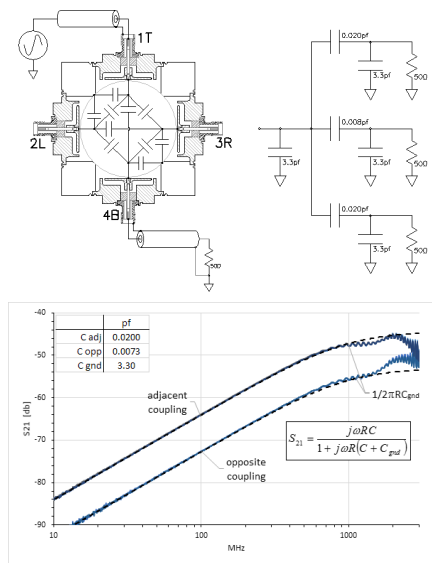


Figure 7:  $S_{21}$  measured between buttons to verify capacitance.

### EFFECT OF $\beta$

With low  $\beta$ , the electric field lines spread out resulting in longer, slower image current, and reduced high frequency content. This effect depends on the proximity to the button and produces a position dependent frequency response. This effect can only be measured with beam or using an electromagnetic field model as  $\beta \approx 1.0$  for a signal traveling along a wire. [9]

As shown in Fig. 8 at injection into the FRIB linac,  $\beta$  equals 0.03275 and the measured position would be 50% too large without correction for  $\beta$  shown in Fig. 9 & 10. By the end of the first linac segment,  $\beta$  equals 0.18647 and the effect is only 2%. The effect is linear near the center of the BPM, as shown in Fig. 11 [6][10].

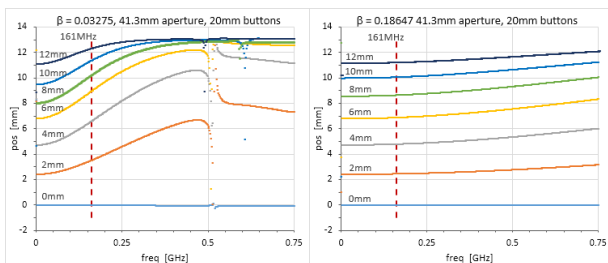


Figure 8: CST calculated position  $(D/\pi)(A-B)/(A+B)$  versus frequency for  $\beta = 0.03275$  and  $0.18647$ . At 0.5 GHz the beam flight time and button diameter are  $1/2$  period.

$$pos \approx \left(\frac{1}{1+G}\right) \frac{D}{\pi} \frac{A-B}{A+B}$$

$$G = 0.0347 \left(\frac{\omega D}{\beta c \gamma}\right)^2 - 0.00181 \left(\frac{\omega D}{\beta c \gamma}\right)^3$$

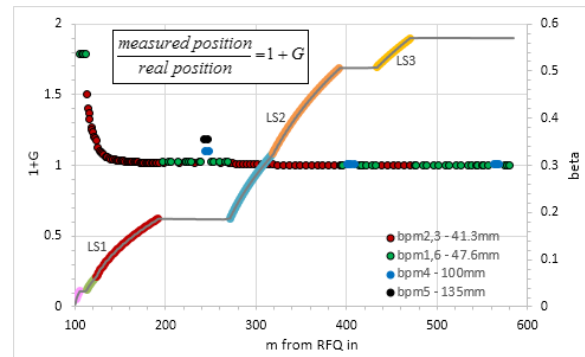


Figure 9: Linear  $\beta$  correction factor for all BPMs in FRIB.

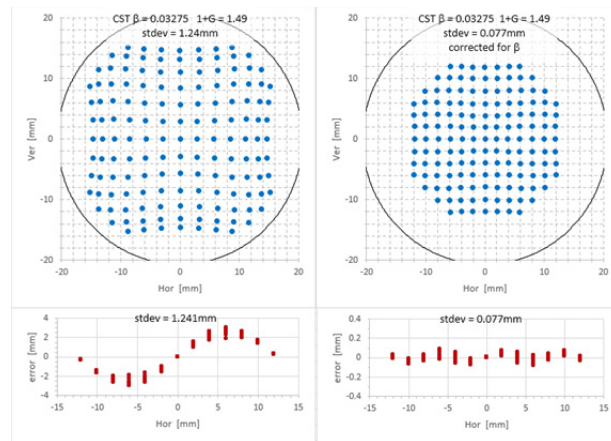


Figure 10: CST model with  $\beta = 0.03275$ . The  $\beta = 1$  polynomial is used to correct linearity. Plot on right uses a polynomial to correct for  $\beta$  before correcting linearity.

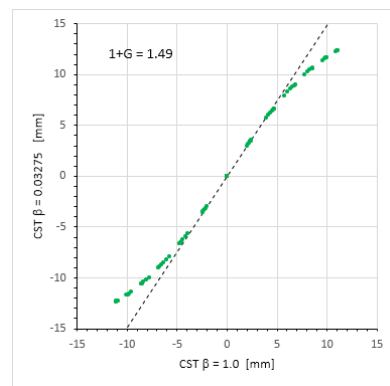


Figure 11: CST model comparing  $\beta = 0.03275$  and  $\beta = 1$ .

### DESIGN DESCRIPTION AND STATUS

The four different BPM designs required for FRIB have nominal apertures of 40, 50, 100, and 150 mm.

#### 40 mm Aperture Design

We moved forward early with the cold 40 mm pick-up design to be prepared to support the cryomodule schedule. The 40 mm aperture BPMs as shown in Fig. 12 include those that will operate at cryogenic temperatures. This design is based on strict cryogenic requirements and interfaces of the device. All stainless steel material will be 316L. The residual magnetic field must be less than 50

mG near the superconducting rf cavities. Four 20 mm SMA buttons are used, one on each face.



Figure 12: 41.3mm ID 20mm diameter button BPM manufactured to FRIB specifications by Solid Sealing Technology.

The axial length is set based on the location of the superconducting cavity and solenoid. Due to a tight clearance between the cavity and solenoid flanges, the BPM needs a bellows to compress roughly .5" for installation. The housing includes a machined flange to avoid extra welds that will throw off the BPM alignment. It will also include through clearance holes that allow for easy installation and cleaning. We will use steel-jacketed SiO<sub>2</sub> cables to connect the BPM to a four-port flange in the vacuum vessel with 50 Ohm feedthroughs with SMA connectors on the vacuum side and N-type connectors airside.

### 50 mm Aperture Design

The 50 mm design will have a similar housing design to the 40 mm design and the same 20 mm buttons. The only difference will be that the housing grows due to the increase in aperture. Two versions will be installed depending on the mechanical interface to the adjacent beam pipe component, so either a beam pipe or a bellows will be welded to the BPM housing.

### 100 mm and 150 mm Aperture Design

The 100 mm aperture BPMs are still in the preliminary stages as shown above in Fig. 13 with two different design variations. One possibility is a housing similar to the 40 and 50 mm apertures using 20 mm buttons. These will include a bellows welded to the housing.

The second design variation has an elliptical aperture to match the beam pipe in two locations of the linac with four split plates with two feedthroughs on top and bottom. [4] The two 150 mm BPMs will likely use this design which may be scaled down for the ten 100 mm BPMs.

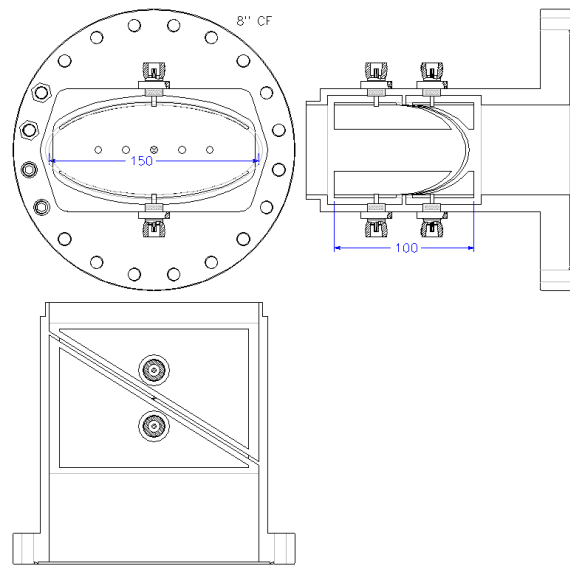


Figure 13: Conceptual design of the 150 mm split plate BPM. Only two are required for FRIB.

### NEXT STEPS

Conceptual designs of the 100 and 150 mm BPMs are complete. Discussion with vendors is required to verify practical realization.

### SUMMARY

Solid Sealing Technologies (SST) helped design, tolerance, and manufacture BPMs using buttons welded to the BPM body that are clean room compatible with superconducting rf cavities and have less than 50 mG residual magnetic field. First articles received are of excellent quality and consistency.

A consistent 1.8% gain error was measured by comparing BPM wire mapping to CST studio model using a particle beam. The difference was partially understood with a 0.8% difference between CST models with a wire and with a particle beam.

The BPM pick-up design meets the physics and mechanical requirements of FRIB and is well understood. The 20 mm button will be used in 135 of the 147 BPMs required. The models and wire measurements demonstrate that polynomials for correction of geometry and low  $\beta$  provide high accuracy and resolution for position, phase, and beam intensity.

### ACKNOWLEDGMENT

We would like to thank Jim Fitzgerald at Fermilab for mapping the BPMs with a wire.

## REFERENCES

- [1] B. Durickovic, D. Constan-Wahl, J. Crisp, G. Kiupel, S. Krause, D. Leitner, S. Nash, R. Rencsok, J. Rodriguez, R. Webber, W. Wittmer, "RF Cavity Phase Calibration Using Electromagnetic Pickups", NA-PAC2013 Proc., Pasadena, USA, 1334, (2013).
- [2] M. Wendt, "Overview of Recent Trends and Developments for BPM Systems", DIPAC2011 Proc., Hamburg, Germany, 18-22, (2011).
- [3] R.E. Shafer, "Beam Position Monitoring", AIP Conf. Proc. 212, 26-58 (1990).
- [4] P. Kowina et al., "Optimisation of 'Shoe-Box Type' Beam Position Monitors Using the Finite Element Methods", DIPAC2005 Proc., Lyon, France, 114-6, (2005).
- [5] C. J. Bouwkamp and N. G. De Bruijn, "The Electrostatic Field of a Point Charge Inside a Cylinder, in Connection with Wave Guide Theory", J. Appl. Phys. 18, 562 (1947).
- [6] A. Lunin, N. Eddy, T. Khabiboulline, V. Lebedev, V. Yakovlev, "Development of a Low-Beta Button BPM for PXIE Project", IBIC2013 Proc., Oxford, UK, 392-5, (2013).
- [7] J. Crisp, D. Constan-Wahl, B. Durickovic, G. Kiupel, S. Krause, D. Leitner, S. Nash, J. A. Rodriguez, T. Russo, R. Webber, W. Wittmer, N. Eddy, C. Briegel, B. Fellenz, D. Slimmer, M. Wendt, "Beam Position and Phase Measurements of Microampere Beams at the Michigan State University ReA3 Facility", NA-PAC2013 Proc., Pasadena, USA, 1187, (2013).
- [8] J. Fitzgerald, J. Crisp, E. McCrory, G. Vogel, "BPM testing, analysis, and correction", AIP Conf. Proc. 451(1), 370-7 (1998).
- [9] P. Kowina, P. Forck, W. Kaufmann, P. Moritz, F. Wolfheimer, T. Weiland, "FEM Simulations – A Powerful Tool for BPM Design", DIPAC2009 Proc., Basel, Switzerland, 35-7, (2009).
- [10] R.E. Shafer, "Beam Position Monitor Sensitivity for Low- $\beta$  Beams", AIP Conf. Proc. 319, 303-8, (1994);